

Electrical Conductivity of a TiO₂ Thin Film Deposited on Al₂O₃ Substrates by CVD

Cheol Seong Hwang* and Hyeong Joon Kim

Dept. of Inorganic Mater. Eng., Seoul National University, Seoul 151-742, Korea

*Samsung Electronics. Co., LTD, Suwon 449-900, Korea.

(Received February 8, 1995)

Electrical conductivity of TiO₂ thin films, deposited on Al₂O₃ substrates by metal organic chemical vapor deposition (MOCVD), was measured by four-point probe method in a temperature range from 800°C to 1025°C and an oxygen partial pressure range from 2.7×10^{-5} atm to 1 atm. In the low oxygen partial pressure region n-type conduction was dominant, but in the high oxygen partial pressure region p-type conduction behavior appeared due to substitution of Ti ions by Al ions, which were diffused from the substrate during post deposition annealing process. Electrical conductivity of the film decreases in the n-type region and increases in the p-type region as the oxygen partial pressure increases. The transition points, which show the minimum conductivity, shifted to the higher oxygen partial pressure region as the measuring temperature increased, but it shifted to lower oxygen partial pressure region with an increase in the post annealing temperature. The results were also discussed with the possible defect models.

Key words : Electrical conductivity, TiO₂ thin films, CVD, Oxygen partial pressure

I. Introduction

TiO₂ is an oxygen deficit nonstoichiometric compound and its degree of nonstoichiometry varies as a function of the surrounding oxygen partial pressure and temperature. Since the electrical conductivity of TiO₂ corresponds to the degree of nonstoichiometry, TiO₂ is an attractive candidate material as the oxygen sensor. Simple operation is the advantage of a TiO₂ oxygen sensor over the galvanic type ZrO₂, which is widely used as the oxygen sensors now. Thin film type oxygen sensors have many advantages over bulk ceramics sensors, such as fast response, easy fabrication process and process reliability et al. However, the electrical conduction mechanism of TiO₂ thin films should be understood before the sensors are used.

Band gap of rutile is 3.0-3.2eV¹⁾ and thus TiO₂ is an electrical insulator at room temperature, but becomes a semiconductor at elevated temperatures. There have been many investigations of the electrical conduction mechanism of TiO₂ by various researchers, but there has not been perfect agreement between their studies.²⁾ This disagreement is mainly due to the existence of an impurity or nonequilibrium atmosphere during sample preparation. Since TiO₂ has 10⁻³ at% nonstoichiometry of oxygen deficiency at 1000°C and oxygen partial pressure of 1 atm,³⁾ the electrical conductivity measurement should be done with pure TiO₂ lower than 10⁻³ at% impurity. In spite of the difficulties, doubly ionized oxygen vacancies, V_O, have been reported to be the major defects of TiO₂ above 800°C in the oxygen partial pressure 1-10⁻⁴atm.⁷⁾ In

case of the TiO₂ thin film the following two conditions are required: first, the electrical resistivity of the substrate should be high enough (about two orders of magnitude higher than that of TiO₂) that the contribution from the substrate to the total electrical conduction is negligible. The high purity polycrystalline Al₂O₃ ceramic may be suitable as a substrate for the TiO₂ thin film.⁴⁾ Second, the solid solubility between thin film and the substrate should be negligible or controllable. No solid-solubility and intermediate phases formation occur between TiO₂ and Al₂O₃ up to 1200°C according to the phase diagram.⁵⁾ However, Sleptys et al.⁶⁾ measured the solid solubility of Al₂O₃ to TiO₂ in the temperature range of 1200-1426°C, 0.62 wt% at 1200°C and 1.97 wt% at 1426°C. Therefore, the heat treatment temperature and duration time will affect the electrical conductivity of TiO₂ thin film because of the diffusion of Al₂O₃ to TiO₂.

II. Experimental Procedure

A 2 μm thick TiO₂ thin film was deposited by a metal organic chemical vapor deposition (MOCVD) process on high purity Al₂O₃ substrate (99.99%) using titanium ethoxide and O₂. The Al₂O₃ substrate had surface roughness smaller than 0.1 μm, and a rectangular shape of 0.6 mm × 5.5 mm × 6 mm. The sample was annealed for 48 hours at 1100°C in air to prevent any variation in the thickness of the film during electrical conductivity measurements and to allow its conversion to the stable rutile phase. Stripe shaped Pt electrodes were formed on the

sample surface using a porous Pt paste (Engelhard #51758 Pt-black). The inter-electrode distance was 0.5 mm. Electrical conductivity of the sample was measured using a DC four-point probe method as a function of oxygen partial pressure, P_{O_2} , and temperature. The oxygen partial pressure was controlled by a proper mixing of high purity oxygen and high purity nitrogen gases, and was measured by an 8% MgO-added zirconia cell. The oxygen partial pressure ranged from 2.7×10^{-5} to 1.0 atm. Because the TiO_2 thin film was polycrystalline, we measured an AC complex impedance, using an impedance analyzer (YHP LF 4192A) as a function of temperature and P_{O_2} to determine the grain boundary effect on conductivity. To determine the electrical conductivity variation due to the variation of Al_2O_3 impurity content in TiO_2 , we annealed the sample at 1050°C, 1100°C, 1170°C, respectively, in air atmosphere for 70 hours, and measured the electrical conductivity as a function of P_{O_2} .

We expect some effect of surface dispersed Pt particles on the electrical conductivity because of the catalytic activity of Pt on the chemical reaction between gas and oxide. A 16.7 wt% H_2PtCl_6 aqueous solution was used to disperse Pt particles on the film surface. The solution was brushed onto the thin film surface, dried at 100°C for 15 minutes and annealed at 1100°C for 2 hours. Pt particles can have different degree of surface catalytic effect according to the specific surface area of the TiO_2 film, and so the following experiments were carried out. From the results of deposition experiments⁵⁾ we know the morphology of a thin film surface can be rough or smooth by changing the deposition conditions, and the different surface morphology can be maintained after heat treatment. Therefore, we prepared the samples with different specific surface areas by controlling the deposition conditions. We made two typical samples with rough and smooth surfaces, and dispersed the Pt particles by the above-mentioned method and measured their electrical conductivity.

III. Results and Discussions

Fig. 1 shows the variation of electrical conductivity of a TiO_2 thin films annealed at 1100°C in air for 48 hours as a function of P_{O_2} (2.7×10^{-5} -1 atm) in the measuring temperature range of 800-1025°C. The slope of the $\ln(\text{conductivity})$ vs. $\ln(P_{O_2})$ curves approaches 1/1.3 when the measuring temperature and P_{O_2} come close to 800°C and 1 atm. It approximates 1/4 at 925°C and $P_{O_2}=1$ atm, but approaches -1/6 as the measuring temperature increases up to 1025°C and P_{O_2} lowers down to 2.7×10^{-5} atm. The change of sign of the slopes in Fig.1 indicates that the conduction mechanism changes from n-type in the low P_{O_2} region to p-type in the high P_{O_2} region. The transition point from n- to p-type conduction, which corresponds to the conductivity minimum point, shifts to a higher oxygen partial pressure region when the measuring temperature increased. An electrolytic region, where

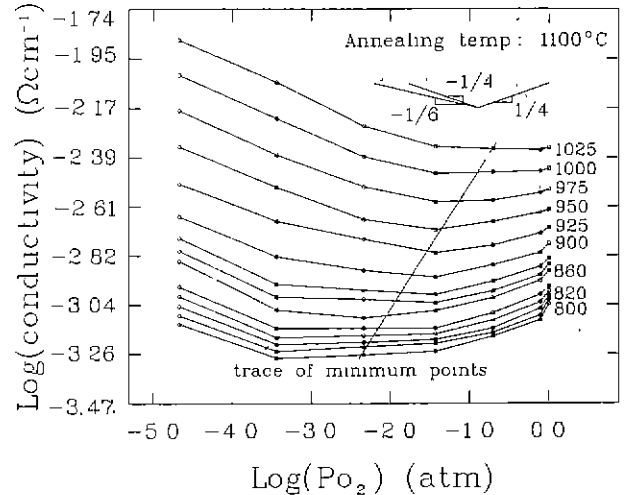


Fig. 1. Electrical conductivity isotherm curves of TiO_2 thin films as a function of oxygen partial pressure

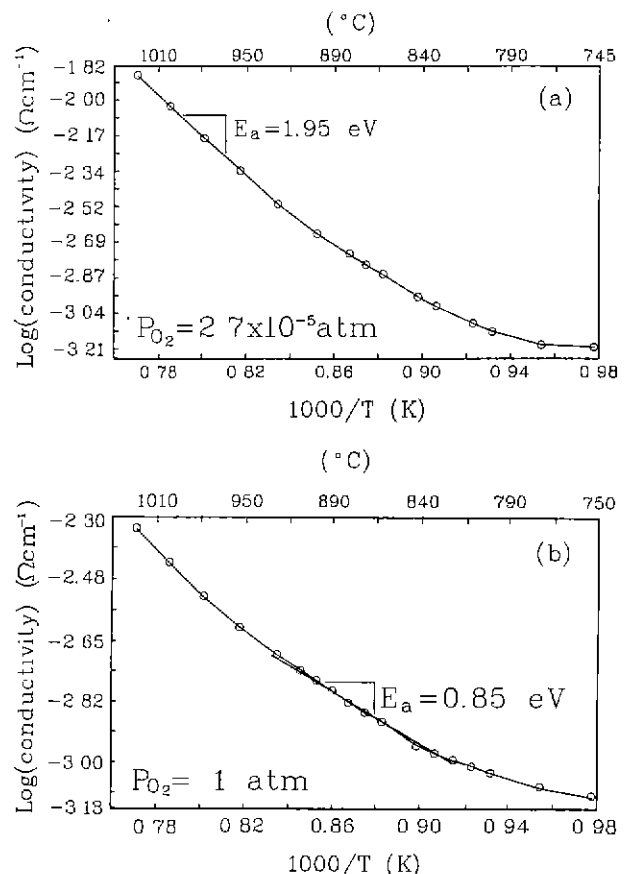


Fig. 2. Variation of electrical conductivity of TiO_2 thin films as a function of $1/T_{measured}$ (a) at $P_{O_2}=2.7 \times 10^{-5}$ atm and (b) at 1 atm.

no change in conductivity occurs with changing P_{O_2} , appears around $P_{O_2}=5 \times 10^{-3}$ atm and $T < 850^\circ C$. The oxygen over the sample enables ionic conduction via oxygen vacancies, because the porous Pt electrode is not a perfect blocking electrode for the oxygen movement. But as the temperature increases the electrical conduction increases

more rapidly and above 900°C the sample shows an electronic semiconductor behavior. Fig. 2(a) and (b) show plots of Ln (conductivity) vs. 1/T data at the different oxygen partial pressures, 2.7×10⁻⁵ atm and 1 atm, respectively. The activation energy in the temperature range of 925-1025°C is about 1.95 eV, as shown in Fig. 2(a), in the low oxygen partial pressure region, in which the n-type conduction is dominant as illustrated in Fig.1. But the activation energy around 870°C is lowered down to 0.85eV in the high oxygen partial pressure region, that is p-type conduction region, as shown in Fig. 2(b).

The following 5 defect equations were postulated, assuming an existence of Al₂O₃ impurities in the TiO₂ thin film :

$$n_i = e' + h \quad K_c = np = n_0^2 = \exp\left(\frac{-E_g}{kT}\right) \quad (1)$$

$$O_o = V_o + \frac{1}{2}O_2 + 2e' \quad K_{ox} = [V_o]n^2Po_2^{1/2} = \exp\left(\frac{-\Delta E_{ox}}{kT}\right) \quad (2)$$

$$Al_2O_3 = 2Al_{Ti}' + V_o'' + 3O_o \quad (3)$$

$$Al_2O_3 = 2Al_i + \frac{3}{2}O_2 + 6e' \quad (4)$$

$$2Al_2O_3 = 3Al_{Ti}' + Al_i'' + 6O_o \quad (5)$$

where e' and h represent free electrons and holes in the crystal, and K_c, K_{ox} and k are reaction constant of electron-hole pair generation by band gap jumping, that of reduction reaction and Boltzman constant, respectively.

Eq.(1) describes a generation of an electron-hole pair. And it is reasonable to assume that Eq.(2) is the redox equation since the major defect type of TiO₂ in the condition of Po₂ > 10⁻⁵ atm and 800-1000°C is V_o. ΔE_{ox} is the activation energy for the redox reaction of the TiO₂ and is 4.58 eV.⁹ Eqs.(3), (4) and (5) are the three possible incorporation equations of the impurity, Al₂O₃, to TiO₂. Except these equations, the following equation can be considered as an incorporation equation of Al₂O₃ to TiO₂.

$$2Al_2O_3 = 4Al_{Ti}' + 6O_o + Ti_i \quad (5-1)$$

But Eq.(5-1) can be ignored since the Ti interstitial is the major defect type of TiO₂ in the region of Po₂ < 10⁻¹⁰ atm,⁷ which is far lower oxygen partial pressure than those employed in this experiment. And we also disre-

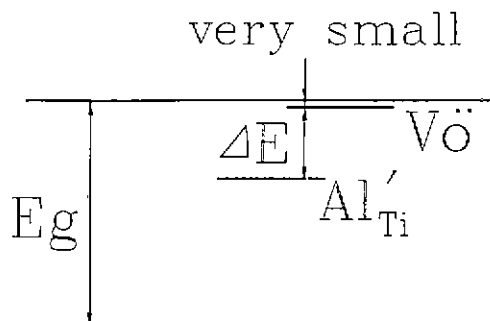


Fig. 3. Schematic band diagram of TiO₂.

gard a contribution of the Schottky or Frenkel defect to electrical conductivity since their effect on electrical conductivity is much smaller than that of nonstoichiometry below 1000°C.

Since the energy level of oxygen vacancy V_o in the TiO₂ crystal lattice is very close to the lower edge of the conduction band, all the generated oxygen vacancies can be ionized to V_o^{••} even at room temperature. However, the Al ion which substitutes Ti ions in the lattice is deep-level impurity, 1 eV lower from the lower edge of conduction band, as illustrated in Fig. 3.¹⁰ Therefore, the ionization process of Al_{Ti} should be regarded as a thermally activated process. Eq. (3-1) and (3-2) are required, in addition to the Eq. (3), to represent the ionization process of Al_{Ti}.

$$2Al_{Ti}' + V_o = 2Al_{Ti}'' + V_o'' \quad (3-1)$$

$$\frac{[Al_{Ti}]^2 [V_o]}{[Al_{Ti}]^2 [V_o]} = \exp\left(\frac{-\Delta E}{kT}\right) \quad (3-2)$$

where ΔE represents the ionization energy of Al ions in TiO₂ and is approximately 1 eV.¹⁰

The electroneutrality equation on the basis of Eqs.(1)-(5) should be

$$n + [Al_{Ti}'] = p + 2[V_o''] + 3[Al_i''] \quad (6)$$

If it is assumed that the electrical conductivity is governed by the electrons generated from Al impurities and the incorporation reaction of Al₂O₃ is dominated by Eq.(3), the electroneutrality Eq.(6) can be simplified as Eq.(7):

$$[Al_{Ti}'] = 2[V_o''] \quad (7)$$

Putting Eq.(7) into Eq.(3-2) and assuming $[Al_{Ti}]=2[V_o]$, Eq.(8) is obtained.

$$[Al_{Ti}'] = [Al_{Ti}] \exp\left(\frac{-\Delta E}{3kT}\right) \quad (8)$$

From Eq.(8) and Eq.(7), we get

$$[V_o''] = \frac{1}{2}[Al_{Ti}] \exp\left(\frac{-\Delta E}{3kT}\right) \quad (8-1)$$

$[Al_{Ti}']$ is the ionized Al concentration in the TiO₂ thin film which is closely correlated to the heat treatment temperature. Therefore, from Eq.(2) and Eq.(8-1) the density of the conduction electron n is given as follows:

$$\begin{aligned} n &= [V_o'']^{-1/2} Po_2^{-1/4} \exp\left(\frac{-\Delta E_{ox}}{2kT}\right) \\ &= \left(\frac{1}{2}\right)^{-1/2} [Al_{Ti}]^{-1/2} Po_2^{-1/4} \exp\left[-\frac{\frac{\Delta E}{6} + \frac{\Delta E_{ox}}{2}}{kT}\right] \end{aligned} \quad (8-2)$$

And the hole density p is given as follows by Eq.(1):

$$p = \left(\frac{1}{2}\right)^{1/2} [Al_{Ti}]^{1/2} Po_2^{1/4} \exp\left[-\frac{\left(E_g - \frac{\Delta E}{6} - \frac{\Delta E_{ox}}{2}\right)}{kT}\right] \quad (8-2)$$

The electron mobility of TiO_2 at room temperature is $0.2 \text{ cm}^2/\text{V}\cdot\text{sec}^{11}$ and an electron moves in the lattice as a small polaron. Bluementhal et al.¹² explained the electron movement in the TiO_2 lattice as a small polaron hopping model and Frederikse¹³ calculated the hopping activation energy as 0.2 eV . Therefore, the electrical conductivity in the n-type conduction region is

$$\begin{aligned} \sigma &\approx \sigma_n = ne\mu_e = ne\mu_e^0 \exp\left(-\frac{\Delta E_h}{kT}\right) \\ &= e[Al_{Ti}]^{-1/2} Po_2^{-1/4} \mu_e^0 \exp\left[-\frac{(\Delta E_h + \frac{\Delta E}{6} + \frac{\Delta E_{ox}}{2})}{kT}\right] \end{aligned} \quad (9)$$

where ΔE_h =hopping energy.

And in the p-type conduction region the conductivity is

$$\begin{aligned} \sigma &\approx \sigma_p = pe\mu_h = pe\mu_h^0 \exp\left(-\frac{\Delta E_h}{kT}\right) \\ &= e[Al_{Ti}]^{1/2} Po_2^{1/4} \mu_p^0 \exp\left[-\frac{(E_g + \Delta E_h - \frac{\Delta E}{6} - \frac{\Delta E_{ox}}{2})}{kT}\right] \end{aligned} \quad (10)$$

under the assumption that the hopping energies of the

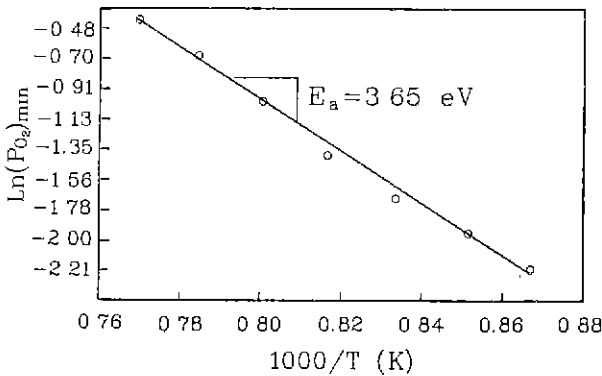


Fig. 4. Variation of electrical conductivity minimum points as a function of $1/T_{\text{measure}}$.

electron and hole is the same. From Eq.(9) and Eq.(10), we can calculate the activation energies for conduction in the n- and p-type conduction regions, respectively. Activation energy for conduction in the n-type conduction region, E_n , is

$$\Delta E_h + \frac{\Delta E}{6} + \frac{\Delta E_{ox}}{2} = 0.2 + \frac{1}{6} + \frac{4.58}{2} = 2.76 \text{ eV} \quad (9-1)$$

And activation energy for conduction in p-type conduction region, E_p , is

$$E_g + \Delta E_h - \frac{\Delta E}{6} - \frac{\Delta E_{ox}}{2} = 3.1 + 0.2 - \frac{1}{6} - \frac{4.58}{2} = 0.94 \text{ eV} \quad (10-1)$$

In summary, we can see from Eqs.(9) and (9-1) that if we assume the impurity incorporation reaction as Eq.(3), the theoretical n-type electrical conductivity has $-1/4$ th power dependance on Po_2 and its activation energy is 2.76 eV in the low Po_2 region. And from Eqs.(10) and (10-1) the theoretical p-type electrical conductivity has $1/4$ th power dependance on Po_2 and its activation energy is 0.94 eV in the high Po_2 region. But the experimental results in Figs. 1 and 2 show that the slope of the graphs approach $-1/6$ as Po_2 decreases in the n-type region and the measured activation energy is far different from the theoretical value. This means that the electrical conduction in this condition is governed not by perfect n-type conduction but the p/n type mixed conduction. This conclusion can be confirmed by the following result. Fig. 4 shows the change in oxygen partial pressure on which the conductivity shows minimum as a function of the measuring temperature. The graph is nearly straight and the activation energy, obtained from the slope, is about 3.65 eV . Since the calculated activation energy of electron conduction is much larger than that of hole, the increase in density of conduction electron with increasing temperature is much larger than that of hole. Therefore, the minimum point of electrical conductivity shifts to higher Po_2 as the measuring temperature in-

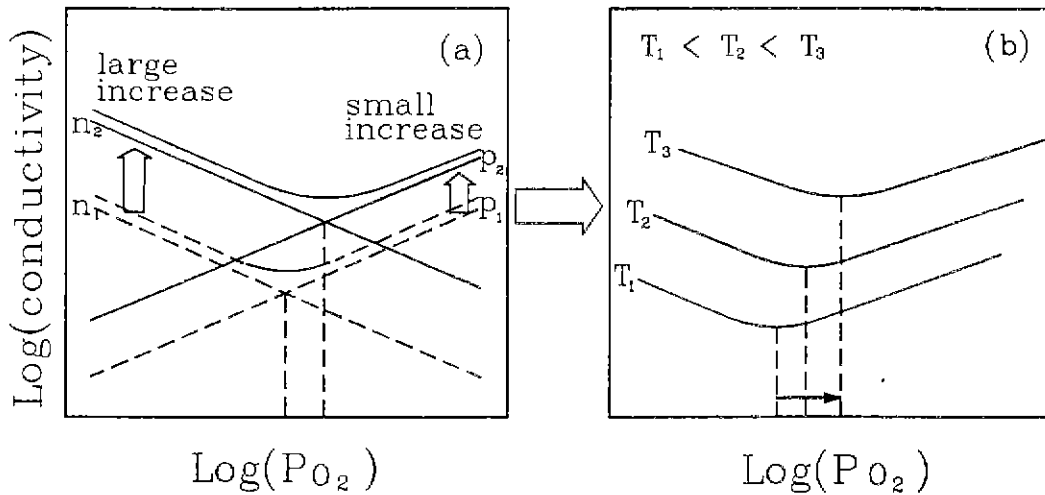


Fig. 5. Effect of measuring temperature on electrical conductivity and its minimum points.

creases. This explanation is shown schematically in Fig. 5(a) and (b). Since the conductivity minimum point coincides with the point of equal value of n- and p-type conductivity, the relationship between the Po₂ and the measuring temperature corresponding to the conductivity minimum is obtained from the following calculation.

$$\begin{aligned}
 ne\mu_n^o \exp\left(-\frac{E_n}{kT}\right) &= pe\mu_p^o \exp\left(-\frac{E_p}{kT}\right) \\
 A\text{Po}_{2\text{min}}^{-1/4} \exp\left(-\frac{E_n}{kT}\right) &= B\text{Po}_{2\text{min}}^{1/4} \exp\left(-\frac{E_p}{kT}\right) \\
 A, B \text{ are constants for given } [Al_n]. \text{ So,} \\
 \text{Po}_{2\text{min}}^{1/2} &= \left(\frac{A}{B}\right) \exp\left[-\frac{(E_n - E_p)}{kT}\right] \\
 \text{Po}_{2\text{min}} &= \left(\frac{A}{B}\right)^2 \exp\left[-\frac{2(E_n - E_p)}{kT}\right] \\
 \ln(\text{Po}_{2\text{min}}) &= 2\ln\left(\frac{A}{B}\right) - \frac{2(E_n - E_p)}{kT} \quad (11)
 \end{aligned}$$

From Eq.(11), we can see that the slope of plot ln (Po_{2min}) vs. 1/T for conductivity minimum points has the value of 2(E_n-E_p)/k. 2(E_n-E_p) in the above theoretical calculation is 3.64 eV, if E_p and E_n are assumed to be 0.94 and 2.76 eV, respectively. The theoretical value is in good agreement with the empirical value, 3.65 eV, obtained from Fig. 4.

The measured electrical conductivity variation in the p-type region is in good agreement with the theoretical value calculated at Po₂=1 atm and T_{measuring}=870°C in Fig. 2(b). But the graph in Fig. 2(b) is not straight but shows curvature at this temperature, and this means that the proposed model can not explain completely the experimental p-type conduction. We suspect that this curvature might originate from the grain boundary effect, so that an AC complex impedance measurements were performed at Po₂=1.0, 1.0×10⁻², 2.2×10⁻³, 1.6×10⁻⁴ atm, and in the temperature range of 800-1025°C. The results show a general behavior at each oxygen partial pressures as follows. As the measuring temperature lowers, the second semicircle due to grain boundary becomes more apparent. But as the measuring temperature increases, the second semicircle shrinks and completely disappears above 1000°C. Even though the second semicircle appears in the low temperature region, it is impossible to separate the second semicircle from the first semicircle and to measure the resistivity of grain itself by the extrapolation method because of the serious overlapping between the semicircles. However, Kilner et al.¹⁵ showed that although the electrical conductivity variation of the grain boundary with temperature is different from that of the grain itself, but the electrical conductivity is usually governed by the conductivity of grain itself in high temperature (1000±200K) region. The common disappearance of second semicircle in high temperature region in the AC complex impedance meas-

urements may be due to the reduction of the effect of grain boundary at high temperature. Therefore, we can regard that the good linearity of Fig. 2 (a), (b) in the high temperature region is due to the grain itself and the curvature in the low temperature region is due to the appearance of the grain boundary effect. The AC complex impedance measurement at Po₂=1 atm and T=920°C shows a small second semicircle. The value of slope, 1/1.3, of plot of Ln (conductivity) vs. Ln (Po₂) about Po₂=1 atm and T=800°C, as shown in Fig. 1, might be resulted from the effect of grain boundary or surface of the thin film on conductivity, but it is difficult to explain the slope theoretically at this point. And this is the reason why the slope of the graph in Fig. 2 (b) in temperatures ranging from 800°C to 900°C was used to calculate the activation energy of p-type conductivity.

Fig. 6 shows the effect of annealing temperature on the electrical conductivity of TiO₂ thin films as a function of oxygen partial pressure and temperature. The electrical conductivity increases as the annealing temperature increases at a given measuring temperature, and the conductivity minimum points shift to lower Po₂ value as the annealing temperature increases at a constant measuring temperature. The minimum point of electrical conductivity shifts to higher Po₂ with an increase in measuring temperature irrespective of annealing temperature. We can also figure out the effect of impurity concentrations on the electrical conductivity from Eqs.(9) and (10). Fig. 7 illustrates that n-type conductivity decreases in the 1/2th power of [Al_n], but the p-type conductivity increases in the 1/2th power of [Al_n]. It also illustrates that the minimum point of electrical conductivity shifts to the lower Po₂ as the impurity concentration increases. Sleptys et al.⁹ have reported that the solid solubility of Al₂O₃ in TiO₂ increases as the annealing temperature increases in the 1200-1426°C range.

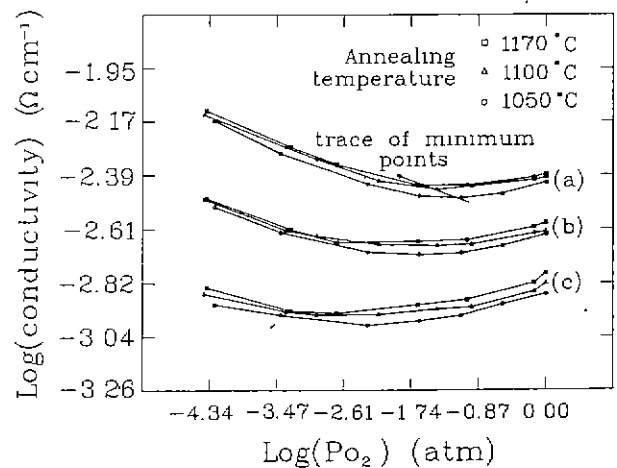


Fig. 6. Variation of electrical conductivity of TiO₂ thin films annealed at different temperatures as a function of oxygen partial pressure at the measuring temperatures (a) 1000°C, (b) 940°C and (c) 860°C.

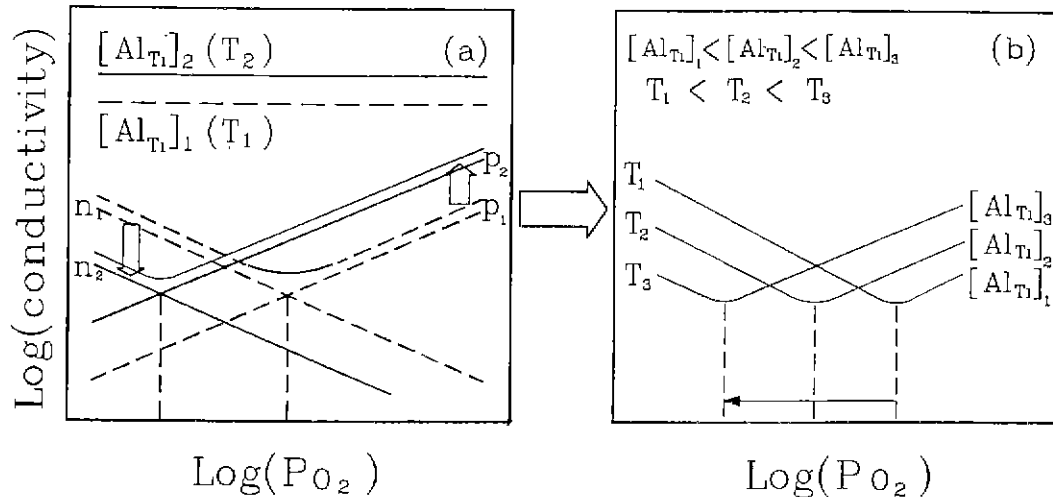


Fig. 7. Effect of annealing temperature (impurity concentration) on electrical conductivity and its minimum point, (a) increased n-type conductivity and decreased p-type conductivity and (b) minimum conductivity point shifts.

Although their experimental temperature range is different from that of this experiment, it can be assumed that the Al_2O_3 impurity content in the TiO_2 thin film increases as the annealing temperature increases. Therefore, as the annealing temperature increases, the impurity concentration and the electrical conductivity increases at a given measuring temperature in the p-type conduction region. Thus the conductivity minimum point shifts to lower Po_2 with an increase in the annealing temperature.

In order to explain the increase of n-type conductivity, we can use Eq.(4) instead of Eq.(3) for the incorporation reaction of Al_2O_3 into TiO_2 , which might be changed by the different Po_2 and temperature. It can be shown from Eq.(4) that three conduction electrons can be generated per one Al interstitial ion. This reaction results in an increase of the n-type conductivity. Especially, this reaction would be dominant in the low Po_2 region, since the evolution of oxygen ions from the TiO_2 can occur during the reaction. Therefore, the increase of the n-type conductivity at low Po_2 region should be ascribed to a change in defect incorporation, i.e. a mixed incorporation mechanism, in which both reactions in Eqs.(3) and (4) are simultaneously occur. It might be assumed that the annealing of the sample at low Po_2 can increase the density of conduction electrons by Eq.(4). Under this assumption we annealed again the air-annealed sample at $\text{Po}_2=2.7 \times 10^{-5}$ atm and $T=1100^\circ\text{C}$ for 70 hours, but could not find any change in electrical conductivity after annealing. We can conclude here that in the low Po_2 region the sample undergoes partial change in defect incorporation mechanism, that is, some of incorporated Al ions occupy the substitutional sites of Ti ions and another does the interstitial sites in the TiO_2 lattice during the conductivity measurements.

Finally we consider the last possible impurity incorporation model expressed by Eq.(5). Sleptys et al.⁶⁾

have explained the solid solubility of Al_2O_3 to TiO_2 by this model. However, the Al_2O_3 impurity cannot affect the conducting electron density according to this model, so that this model can not explain the results of this experiment. This discrepancy may have resulted from different temperature ranges, that is, Sleptys et al. performed their experiment in the high temperature region of $1200\text{-}1426^\circ\text{C}$ whilst our experiment was done in the region of $800\text{-}1025^\circ\text{C}$.

Fig. 8(a) and (b) show the effect of surface-dispersed Pt particles on electrical conductivity of the smooth-surface (root mean square roughness of less than $0.1 \mu\text{m}$) and the rough-surface (root mean square roughness of larger than $1 \mu\text{m}$) TiO_2 thin films, respectively, as a function of measuring temperature. Electrical conductivity of smooth surface thin film with Pt particles is smaller than that without Pt particles, as shown in Fig. 8(a). But with rough-surface thin film electrical conductivity of bare surface is smaller than that with Pt particles, as shown in Fig. 8(b). We can explain the electrical conductivity decrease in n-type semiconducting TiO_2 thin films shown in Fig. 8(a) using the "electron pumping effect" of Pt particles. The electrons move from TiO_2 thin film to Pt particles owing to the work function difference, and the Pt particles capture the electrons from the TiO_2 thin film. The captured electrons can not contribute to electrical conduction because the dispersed particles are separated from each other, and this phenomenon results in a decrease in the electrical conductivity. Akubuiro et al.¹⁶⁾ also reported the same effect of Pt particles for the sintered TiO_2 sample doped with cations of different valency. However, results in Fig. 8(b) can not be explained by the electron pumping effect. This increase in electrical conductivity can be understood by the chemical effect of Pt particles. Akubuiro et al.¹⁹⁾ also measured the electrical conductivity of Pt particle dispersed TiO_2 ceramics under H_2 atmosphere, and they compared the

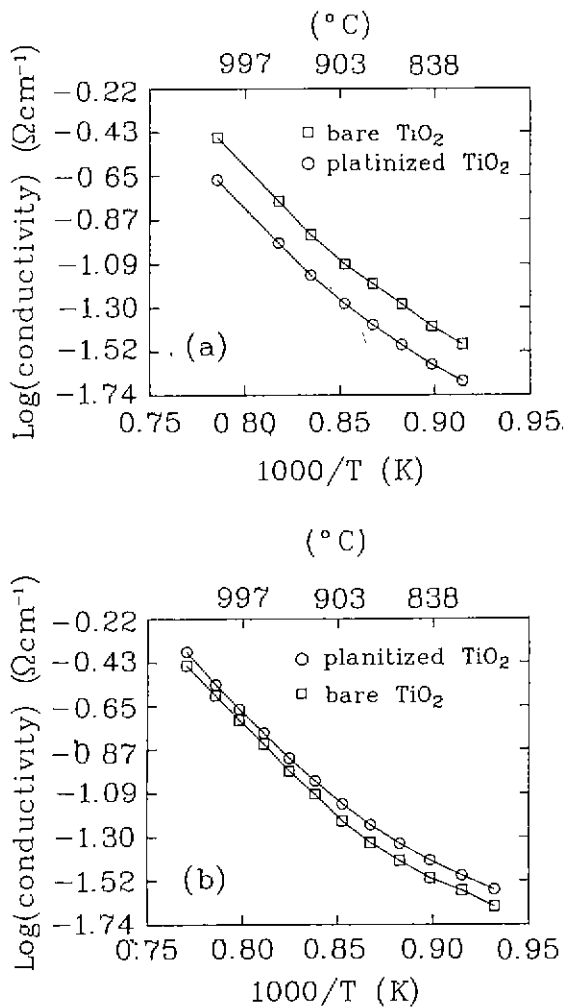


Fig. 8. Effect of Pt particles on electrical conductivity as a function of $1/T_{\text{measure}}$: (a) smooth surface sample and (b) rough surface sample.

results with that of TiO₂ ceramics without Pt particles. They found that the Pt particle dispersed sample had a greater electrical conductivity. They explained the result as follows. H₂ molecules are dissociatively adsorbed on Pt particles as H⁺ ions. These adsorbed H⁺ ions migrate to TiO₂ thin film and react with the lattice oxygen ions. This reaction can generate H₂O or OH and leaves oxygen vacancy and conduction electrons in the TiO₂ ceramics which increases the electrical conductivity. We assume that the electrical conductivity of the rough-surface TiO₂ thin film increases by the dissociative adsorption of N₂ on Pt particles. The rough-surface TiO₂ thin film has a much larger surface-to-volume ratio than the smooth-surface sample, and the surface catalytic effect of Pt particles on electrical conductivity overcomes the electron pumping effect of the Pt particles. It can also be shown from Fig. 8(b) that the conductivity increase effect becomes relatively small as the measuring temperature increases. As the temperature increases, the conduction electron density in the thin film increases by a thermal

activation process and thus the electron density increase by the surface catalytic effect of Pt particles is screened by the thermal effect. So the effect of an electrical conductivity increase due to Pt particles is smaller as the measuring temperature increases. The electron pumping effect and the Pt catalytic effect of N₂ on electrical conductivity may be more effective because the TiO₂ sample has a thin film form.

IV. Conclusions

The electrical conductivity of a TiO₂ thin film deposited on Al₂O₃ substrate varies as a function of Po₂ and the temperature, and the variations can be explained theoretically by assuming that the major defect type of TiO₂ thin film is doubly ionized oxygen vacancies. The sample shows an electrical conduction type transition, from n-type to p-type as the oxygen partial pressure increases, due to the Al impurity ions diffused from the substrate. The electrical conductivity changes with changing the heat treatment temperature, i.e., the Al impurity ion concentration. The incorporated Al ions mainly substitute the lattice Ti ion and hence increase the p-type conduction. Some portion of Al ions exist as interstitial ions, Al_i, in the low Po₂ region and increase the n-type conduction. Grain boundaries seem to contribute to the electrical conduction as the temperature goes down and the oxygen partial pressure increases. Pt particles dispersed on the smooth-surface samples causes an electrical conductivity decrease, but they increase the electrical conductivity in the case of a rough-surface sample. This behavior can be explained by the electron pumping effect and the surface catalytic effect of Pt particles on dissociative adsorption of N₂.

Acknowledgement

The authors acknowledge the financial support of this work by the Korea Science & Engineering Foundation and the Electronics and Telecommunications Research Institute.

References

1. W. D. Kingery, H. K. Bowen and D. R. Uhlmann, "Introduction to Ceramics," 2nd Ed., p. 868, A Wiley Interscience Co., NY, 1976.
2. P. Kofstad, "Oxides of Group IVA Elements" in "Nonstoichiometry, Diffusion, and Electrical Conductivity in Binary Metal Oxides," pp. 137-48, A Wiley Interscience Co., NY, 1972.
3. *ibid*, p 143.
4. W. D. Kingery, H. K. Bowen and D. R. Uhlmann, "Introduction to Ceramics," 2nd Ed., pp. 907, A Wiley Interscience Co., NY, 1976.
5. A. M. Lejus, D. Goldberg and Revcolevschi, "Phase Diagrams for Ceramists," Vol. 3., Edited by E. M. Levin, C. R. Robbins, and H. F. McMurdie, p. 135, American

- Ceramic Society, Columbus, OH, 1975.
6. R. A. Sleptys and D. A. Vaughan, "Solid Solution of Aluminium Oxide in Rutile Titanium Dioxide," *J. Phys. Chem.*, **73** [7] 2157 (1969).
 7. B. K. Kim, "Study of the Time Dependant Electrical Conductivity of Rutile Single Crystal" (in Kor.) ; M. S. Thesis, Seoul National University, Seoul, Korea, 1988.
 8. C. S. Hwang and H. J. Kim, "Effect of Deposition Conditions on Deposition Mechanism and Surface Morphology of TiO_2 Thin Films Deposited by Chemical Vapor Deposition"; pp. 437-56 in *Ceramic Transactions, Vol. 15, Materials and Processes for Microelectronic Systems*, Edited by K. M. Nair, R. Pohanka, and R. C. Buchanan, American Ceramic Society, Westerville, OH, 1990.
 9. P. Kofstad, "Oxides of Group IVA Elements" in "Nonstoichiometry, Diffusion, and Electrical Conductivity in Binary Metal Oxides," p. 142, A Wiley Interscience Co., NY, 1972.
 10. J. Pennewiss and B. Hoffmann, "Electrical Conductivity of Aluminium-Doped TiO_2 Ceramic After Quenching," *Mater. Letters*, **5** [4] 121 (1987).
 11. R. N. Blumenthal, J. Coburn, J. Baukus and W. M. Hirthe, "Electrical Conductivity of Nonstoichiometric Rutile Single Crystals from 1000°C to 1500°C," *J. Phys. Chem. Sol.*, **27** 643 (1966).
 12. R. N. Blumenthal, J. Baukus and W. M. Hirthe, "Studies of the Defect Structure of Nonstoichiometric Rutile, TiO_{2-x} ," *J. Electrochem. Soc.*, **114** [2] 172-76 (1967).
 13. H. P. R. Frederikse, "Recent Studies on Rutile(TiO_2)," *J. Appl. Phys. Suppl.*, **32** [10] 2211-15 (1961).
 14. H. L. Tuller, "Mixed Conduction in Nonstoichiometric Oxides" in "Nonstoichiometric Oxides," pp. 271-335, Edited by O. T. Sorensen. Academic Press, London, UK, 1981.
 15. J. A. Kilner and B. C. H. Steele, "Mass Transport in Anion Deficient Fluorite Oxides" in "Nonstoichiometric Oxides," pp. 233-269, Edited by O. T. Sorensen. Academic Press, London, UK, 1981.
 16. E. C. Akubuiro and X. E. Verykios, "Effects of Al-tervalent Cation Doping on Electrical Conductivity of Platinized Titania," *J. Phys. Chem. Sol.*, **50** [1] 17-26 (1989).